

# TARGETING FAULTY BEARINGS FOR AN OCEAN TURBINE DYNAMOMETER

by:

*Nicholas Waters, Dr. Pierre-Philippe Beaujean, and Dr. Dave Vendittis*

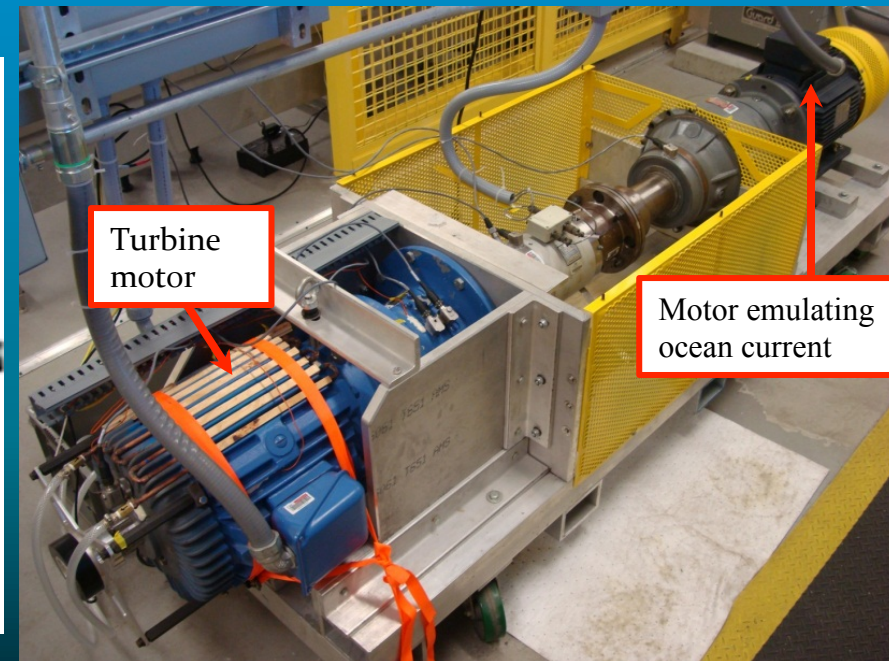
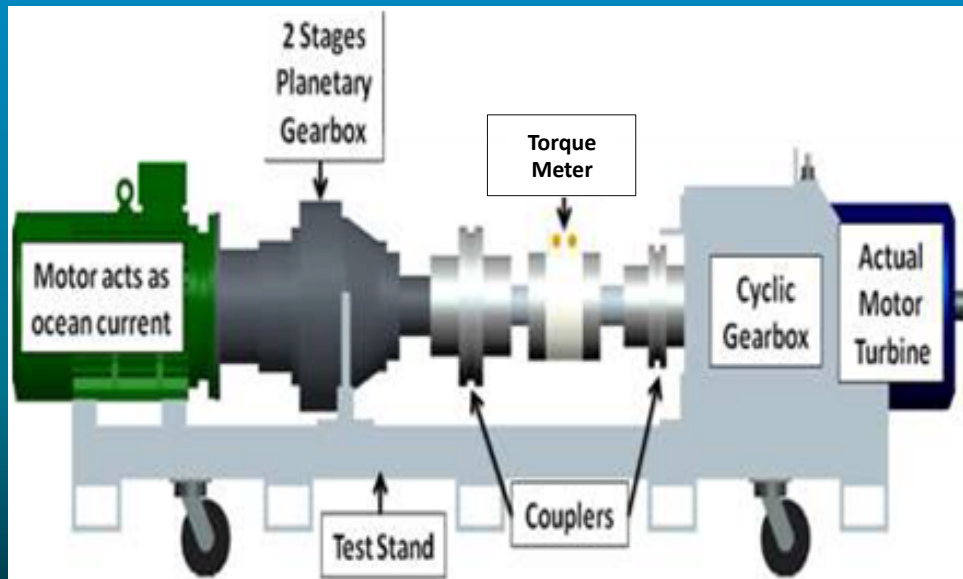
## Outline

---

- **Abstract.**
- **Background on bearing fault detection.**
- **Simplified mathematical model describing the vibrations produced by a bearing with a single raceway defect.**
- **Overview of the signal processing techniques involved and the approach to detecting, localizing, and identifying bearing faults occurring on the dynamometer in real time.**
- **Analysis of data collected from a controlled lathe experiment and data collected over the course of a month leading up to a fault in the dynamometer.**
- **Conclusion**

## Abstract

- Real-time, vibrations-based condition monitoring method
- Detection, localization and identification of bearing faults occurring on a dynamometer
- Dynamometer prototype for ocean turbine
- Method demonstrated on controlled lathe setup with a single faulty bearing
- Data leading up to fault on dynamometer processed to reveal outer race bearing defect



## Introduction

---

- **Vibration condition monitoring proven effective and universally accepted method for machine condition monitoring.**
- **A LabVIEW application, Smart Vibrations Monitoring System (SVMS), designed for autonomous online monitoring operational health of dynamometer.**
- **SVMS computes a range of parameters (power spectral density, fractional octave, kurtosis, cepstrum, time waveform, and more)**
- **The long term goal of the SVMS - use it for online monitoring of the actual ocean turbine once it is deployed.**
- **The purpose of this research - add the ability to specifically target bearing related defects occurring on the dynamometer, to SVMS.**

## Scientific Approach

- As a first approach to modeling the vibrations induced by bearing raceway defects, we first consider the vibrations caused by a single ball bearing rolling over a single defect in the inner raceway.

- The parameters are defined as follows:

$\bar{q}_0$  = loading due to the mass of the shaft and bearing.

$\theta$  = angle measured from the vertical to the center of the defect.

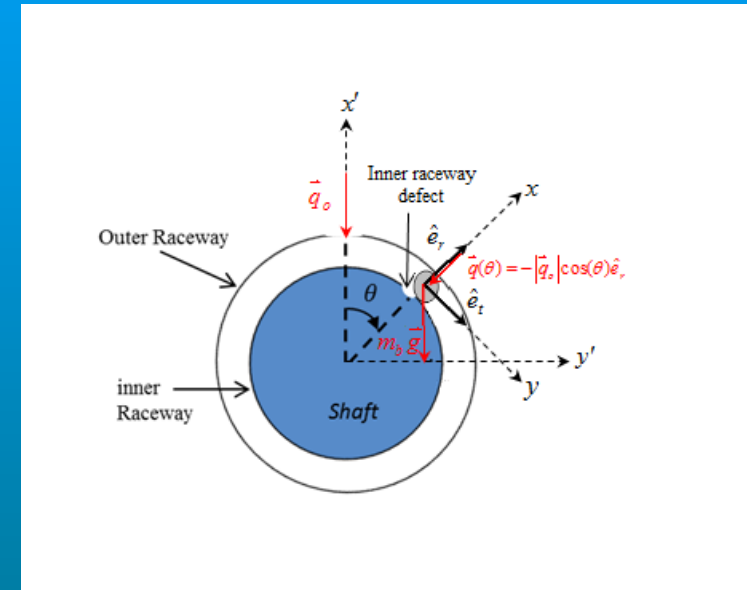
$m_b \bar{g}$  = force due to gravity acting on the mass of the ball.

$\hat{e}_r, \hat{e}_t$  = radial and tangential vectors of unit magnitude, in the x and y directions.

$\bar{q}(\theta)$  = the projection of the shaft and bearing loading, on the rotated x,y-coordinate system.

- Assumptions:

- There is no shaft imbalance and the loading from the shaft acts vertically downward, attaining a maximum of  $q_0$  along the  $x'$  axis.
- There is only a single defect along the inner raceway.



## Scientific Approach

- Through analysis of the equivalent lumped parameter model, we find the displacement for a single impact and mode of vibration  $n$ ,

$$x_n(t) = X_n e^{-\omega_{0,n} \zeta_n t} \cos(\omega_{d,n} t - \phi_{0,n}) u(t). \quad (1)$$

- The parameters are defined as follows:

$X_n$  = amplitude of the displacement for mode  $n$  at time  $t = 0$ .

$\omega_{0,n}$  = natural angular frequency.

$\zeta_n$  = damping ratio (we assume  $\zeta_n = 1$  since the system is underdamped).

$\omega_{d,n}$  = damped natural angular frequency.

$\phi_{0,n}$  = initial phase for mode of vibration  $n$ .

$$u(t) = \begin{cases} 1 & \text{for } t \geq 0 \\ 0 & \text{otherwise} \end{cases} \quad (\text{introduced since the system is causal}).$$

## Scientific Approach

- Assuming that every ball is identical, and accounting for all the modes of vibration and impacts,

$$x(t) = \sum_{n=1}^{N_s} \sum_{k=-\infty}^{\infty} X_n(kT_d) e^{-\omega_{0,n}\zeta_n(t-kT_d)} \cos[\omega_{d,n}(t-kT_d) - \phi_{0,n}(kT_d)] u(t-kT_d). \quad (2)$$

- The parameters are defined as follows:

$T_d$  = period of rotation for a single ball.

$KT_d$  = time delay associated with the  $k^{\text{th}}$  impact.

$N_s$  = total number of modes of vibration.

- Differentiating (2) twice, we find the acceleration,

$$a(t) = \sum_{n=1}^{N_s} \sum_{k=-\infty}^{\infty} A_{n,k} e^{-\omega_{0,n}\zeta_n(t-kT_d)} \cos[\omega_{d,n}(t-kT_d) - \phi'_{0,n}(kT_d)] u(t-kT_d), \quad (3)$$

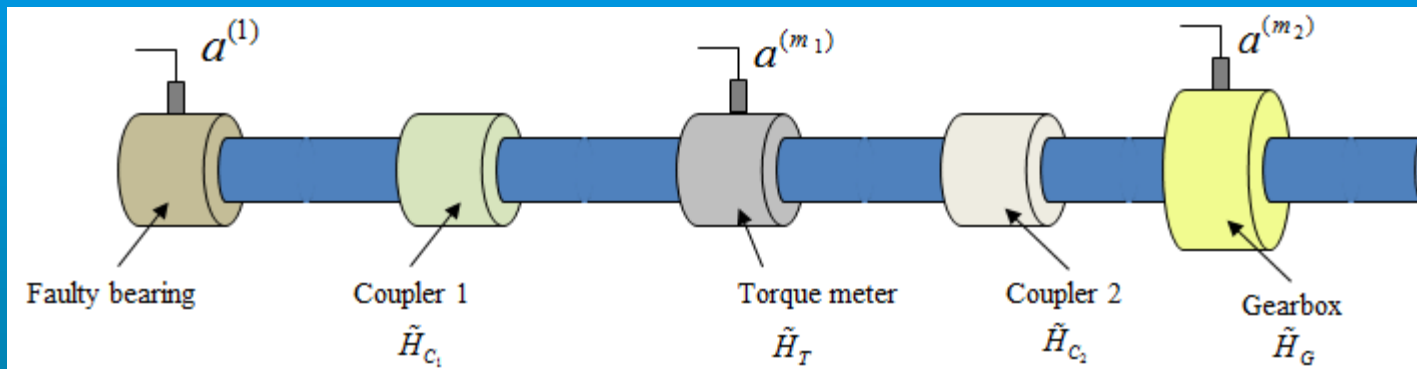
where

$A_{n,k}$  = maximum observed acceleration.

$\phi'_{0,n}$  = initial phase associated with the acceleration for mode of vibration  $n$ .

## Scientific Approach

- Equation (3) assumes that the accelerometer is placed directly over the source of vibrations since there is no term to account for signal degradation in the vibrations as these vibrations propagate through the structure.



- Let  $\tilde{H}_{C_1}$ ,  $\tilde{H}_T$ ,  $\tilde{H}_{C_2}$ , and  $\tilde{H}_G$  represent the complex loss coefficients (or transfer functions) associated with the faulty bearing, first coupler, torque meter, second coupler, and gearbox, respectively.
- We introduce the superscript notation,  $a^{(1)}$  to represent the accelerometer placed directly over the faulty bearing and  $a^{(m_i)}$  (for  $i = 1, 2, \dots, 6$ ) to represent the accelerometer placed a distance  $d_{m_i}$  from the faulty bearing.

## Scientific Approach

- For the acceleration measured at location  $m_i$  on the dynamometer, we let  $\beta^{(m_i)}$  represent the frequency response of the modal attenuation of the vibrations as they propagate through the structure,

$$\beta^{(m_i)} = e^{-\omega_{d,n}\xi_n\tau_{d,n}^{(m_i)}} \tilde{H}^{(m_i)}. \quad (4)$$

- In the above equation,

$$\tilde{H}^{(m_i)} = \begin{cases} \tilde{H}_{C_1} \cdot \tilde{H}_T, & \text{for } i = 1 \\ \tilde{H}_{C_1} \cdot \tilde{H}_T \cdot \tilde{H}_{C_2} \cdot \tilde{H}_G, & \text{for } i = 2 \end{cases}. \quad (5)$$

- Since we are dealing with narrow band portions of the signal, we simply find an average value for impulse response of  $\beta^{(m_i)}$  through measurements.
- Equation for acceleration for single mode of vibration

$$a_n^{(m_i)}(t) = \sum_{n=1}^{N_s} \sum_{k=-\infty}^{\infty} \beta_n^{(m_i)} A_{n,k}^{(1)} e^{-\omega_{d,n}\xi_n(t-kT_d)} \cos \left[ \omega_{d,n}(t-kT_d) - \phi_n^{(1)}(kT_d) \right] u(t-kT_d), \quad (6)$$

- Thus, accounting for signal degradation in the vibrations observed at location  $m_i$ , the maximum observed acceleration will be  $\beta_n^{(m_i)} A_{n,k}^{(1)}$ .

## Signal Processing: Power Spectral Density and Coherency

- We let  $r^{(m_i)}(t)$  denote the measurement equivalent of  $a^{(m_i)}(t)$ .
- We estimate the one-sided Power Spectral Density (PSD) of  $r^{(m_i)}(t)$  (written as  $\hat{G}_{r^{(m_i)}}(\omega)$ ), through block averaging (Welch algorithm), using Blackman windows and 50% overlap.

- Estimate coherency between the accelerometer outputs  $r^{(m_i)}(t)$  and  $r^{(m_j)}(t)$ ,

$$\hat{\gamma}_{r^{(m_i)}r^{(m_j)}}(\omega) = \frac{|\hat{G}_{r^{(m_i)}r^{(m_j)}}(\omega)|^2}{\hat{G}_{r^{(m_i)}}(\omega)\hat{G}_{r^{(m_j)}}(\omega)} \quad (7)$$

- $\hat{G}_{r^{(m_i)}r^{(m_j)}}(\omega)$  is the one-sided Cross Spectral Density (CSD) between the accelerometer outputs  $r^{(m_i)}(t)$  and  $r^{(m_j)}(t)$ .
- The coherency ranges between 0 and 1.
- Coherency value of 1 = high correlation (or dependency) between these two signals for this given frequency band.

## Signal Processing: Power and Confidence Interval

- For each day of data acquisition and for each accelerometer, the estimated average power is calculated within every predetermined frequency band  $\omega_n - \frac{\Delta\omega_n}{2} \leq \omega \leq \omega_n + \frac{\Delta\omega_n}{2}$ .

$$\bar{\Pi}_n^{(m_i)} = \frac{1}{\Delta\omega_n} \int_{\omega_n - \frac{\Delta\omega_n}{2}}^{\omega_n + \frac{\Delta\omega_n}{2}} \hat{G}_{r^{(m_i)}}(\omega) d\omega. \quad (8)$$

- The confidence interval at  $1 - \alpha$  confidence level for this average power estimate is

$$1 - \alpha = \Pr \left[ \frac{v \bar{\Pi}_n^{(m_i)}}{\chi^2_{\frac{1-\alpha}{2}, v}} \leq \bar{\Pi}_n^{(m_i)} \leq \frac{v \bar{\Pi}_n^{(m_i)}}{\chi^2_{\frac{\alpha}{2}, v}} \right]. \quad (9)$$

- The parameters in (9) are defined as follows:

$\bar{\Pi}_n^{(m_i)}$  = true average power across the frequency band.

$v = K'_w Q$  (degrees of freedom).

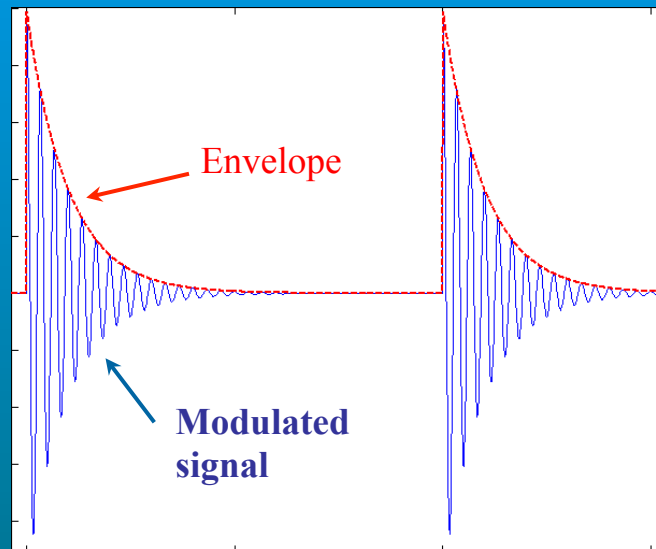
$K'_w$  = window scaling factor.

$Q$  = number of block averages used to estimate  $\hat{G}_{r^{(m_i)}}(\omega)$ .

$\chi^2$  = chi-square distribution.

## Signal Processing: Envelope Analysis

- The envelope of the acceleration measured at accelerometer  $m_i$  for mode  $n$  is of the form  $\beta_n^{(m_i)} A_{n,k}^{(1)} e^{-\omega_{0,n}\xi_n(t-kT_d)} u(t-kT_d)$ .
- The envelope contains valuable information regarding the time signature of every mode as a function of the sensor location.



- The Hilbert transform filters are used to isolate the envelope of individual modes for each acquired signal (demodulation of the signal) .
- From the envelope, periodicity due to balls coming in contact with the defect are highlighted and allow for identification of the faulty bearing.

## Methodology: Impulse response and frequency selection

---

- **Frequency bands for fault detection are selected.**
- **System is excited and impulse response is studied.**
- **PSD is plotted for array of accelerometers.**
- **The frequency bands are then selected based on the following criteria:**
  - i. **The frequency band is preferably located in the upper frequency range to (a) avoid low frequency interferences (b) accentuate the high frequency attenuation of a signal.**
  - ii. **The frequency band shows high coherency (equation (7)) between accelerometers (i.e. the coherency is close to 1).**
  - iii. **If possible, the frequency band isolates a single peak in the PSD.**
  - iv. **Observe a decrease in in-band power across the array of accelerometers as the distance from the strike to the accelerometer increases.**
  - v. **The frequency band contains sufficient damping (determined from envelope).**

## Methodology: Envelope Power & Thresholding

- The envelope power is computed as an instantaneous power from the analytic signal:

$$\Pi_n^{(m_i)}(t) = \frac{|\tilde{r}_n^{(m_i)}(t)|^2}{T_s}, \quad (12)$$

- Envelope power is thresholded based on accelerometer placement and isolated mode(s) of vibration.
- Thresholds are determined based on envelope power levels assuming healthy operational conditions for the dynamometer.

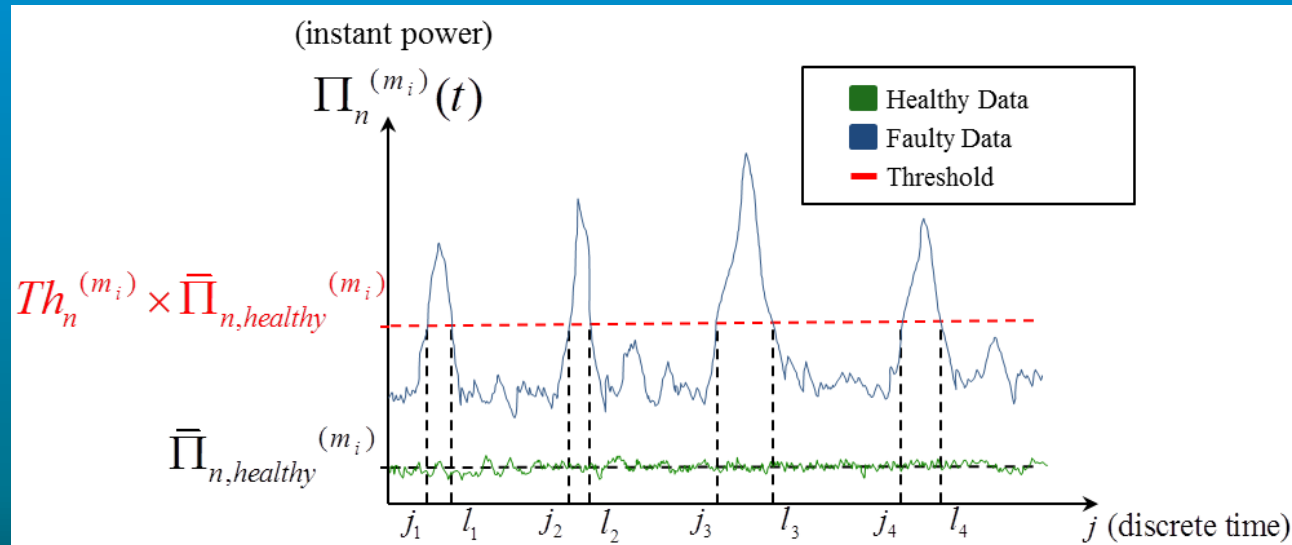
$$\Pi_{n,healthy}^{(m_i)}(t) < Thr_n^{(m_i)} \times \bar{\Pi}_{n,healthy}^{(m_i)} \quad \forall t, \quad (13)$$

where

$$\bar{\Pi}_{n,healthy}^{(m_i)} = E \left[ \frac{|\tilde{r}_{n,healthy}^{(m_i)}(t)|^2}{T_s} \right]. \quad (14)$$

## Methodology: Detection (Envelope Power)

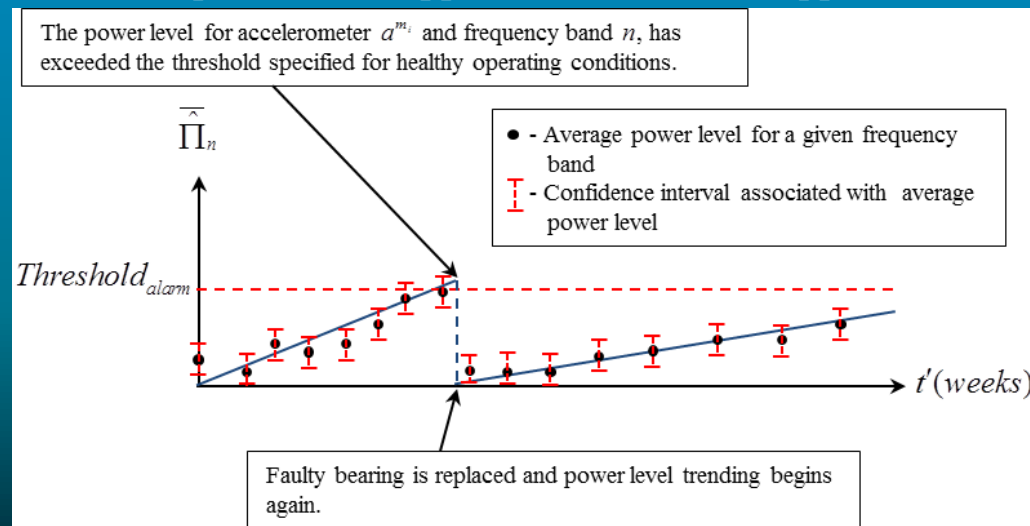
- For each envelope that isolates mode(s) of vibration  $n$ , the envelope power is computed across the array of accelerometers.
- Each accelerometer's envelope power is plotted against its respective envelope power threshold for the isolated mode(s) of vibration,  $Th_n^{(m_i)} \times \bar{\Pi}_{n,healthy}^{(m_i)}$ .
- Envelope power levels that exceed the thresholds are averaged to obtain the average excess power level per time that exceeds the threshold, denoted  $\bar{\Pi}_{n,exceed}^{(m_i)}$ .



$$\bar{\Pi}_{n,exceed}^{(m_i)} = \frac{\sum_{j=j_1}^{l_1} |\tilde{r}_n^{(m_i)}(t)|^2 + \sum_{j=j_2}^{l_2} |\tilde{r}_n^{(m_i)}(t)|^2 + \dots + \sum_{j=j_4}^{l_4} |\tilde{r}_n^{(m_i)}(t)|^2}{[(l_1 - j_1 + 1) + (l_2 - j_2 + 1) + \dots + (l_4 - j_4 + 1)] T_s} \quad (15)$$

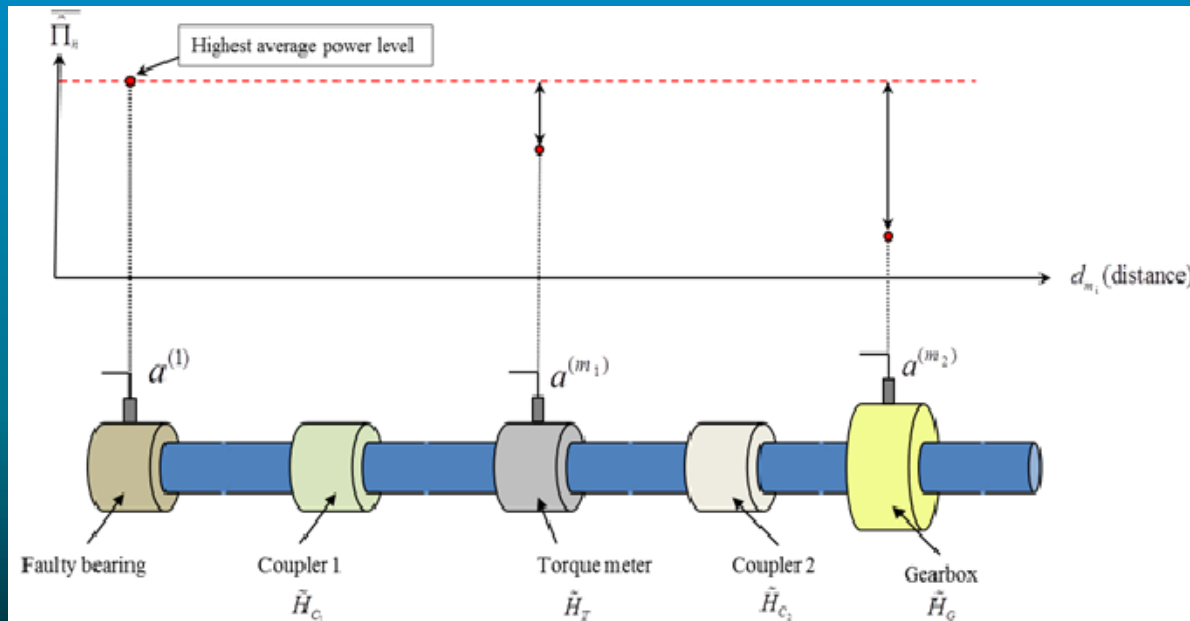
## Methodology: Detection

- Performed once the dynamometer reaches steady state for a given shaft rotational speed.
  - i. The average power level within every predetermined frequency band is computed across the array of accelerometers, along with the confidence intervals .
  - ii. Each average power level is compared to its respective baseline average power level for the given shaft rotational speed.
  - iii. Measurements are repeated over the course of weeks to determine whether the power levels across any of the frequency bands increases for any of the accelerometers over time.
  - iv. If an upward trend in the power levels for any of the frequency bands appears across at least the majority of accelerometers and if the power levels approach or exceed an upper threshold, then there is a fault occurring.



## Methodology: Localization

- Localization refers to determining the proximity of the faulty bearing location to the accelerometer placement.
- Performed once the dynamometer reaches steady state for a given shaft rotational speed.
  - i. The power levels across specific frequency bands are averaged for each accelerometer.
  - ii. If an accelerometer acquires data with the highest average power level across a frequency band and if for the same frequency band, the remaining accelerometers show a decrease in average power levels as their distance increases, then this accelerometer is closest to the defect.

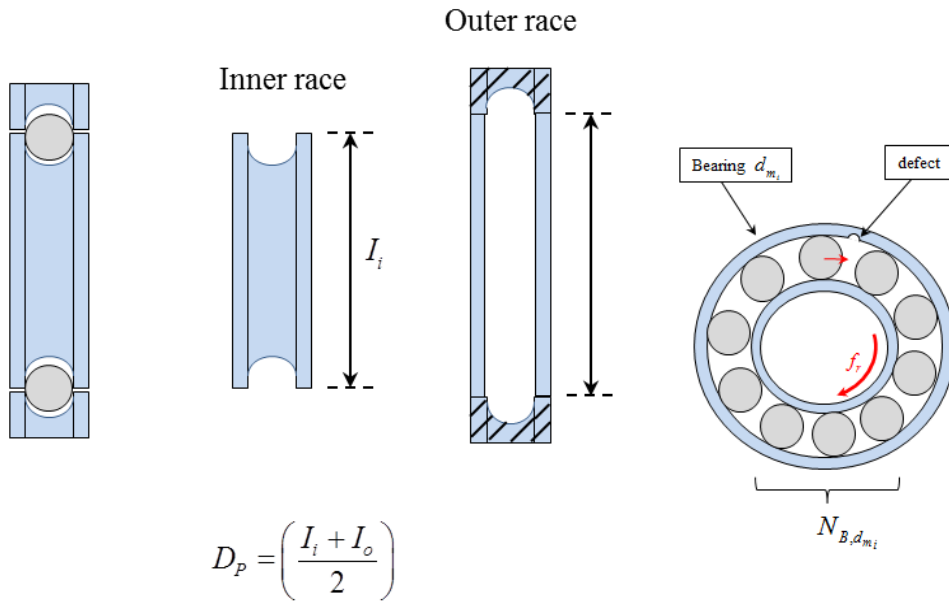


## Methodology: Identification

---

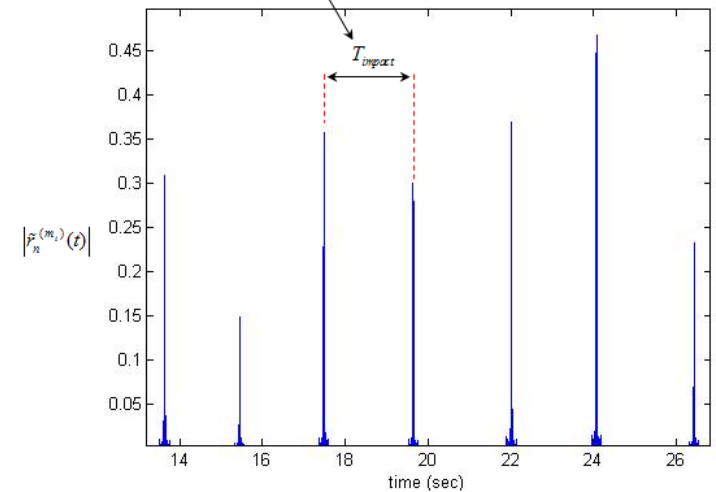
- **Identification refers to determining the exact bearing containing the raceway defect.**
  
- **Performed once the dynamometer reaches steady state for a given shaft rotational speed.**
  - i. **Envelope analysis on the acquired vibration signals is performed within the specified frequency bands and across the array of accelerometers.**
  
  - ii. **From the envelope, we can attain the period between impacts.**
  
  - iii. **We calculate the theoretical fault frequencies due to an inner or outer raceway defect for each of the bearings and for the shaft rotational speed.**
  
  - iv. **The impact frequency should correspond to one of the fault frequencies for one of the bearings and the shaft rotational speed.**

## Methodology: Identification



$$\frac{N_{B,d_{m_i}}}{2} f_r \left( 1 - \frac{D_{B,d_{m_i}}}{D_{P,d_{m_i}}} \right) = f_{o,d_{m_i}} \quad \frac{N_{B,d_{m_i}}}{2} f_r \left( 1 + \frac{D_{B,d_{m_i}}}{D_{P,d_{m_i}}} \right) = f_{i,d_{m_i}}$$

$$f_{o,d_{m_i}} \approx \frac{1}{T_{\text{impact}}} \quad f_{i,d_{m_i}} \neq \frac{1}{T_{\text{impact}}}$$



- The parameters for the figures are defined as follows:

$N_{B,d_{m_i}}$  = number of balls in bearing.

$D_{P,d_{m_i}}$  = Ball pitch diameter.

$D_{B,d_{m_i}}$  = Ball diameter.

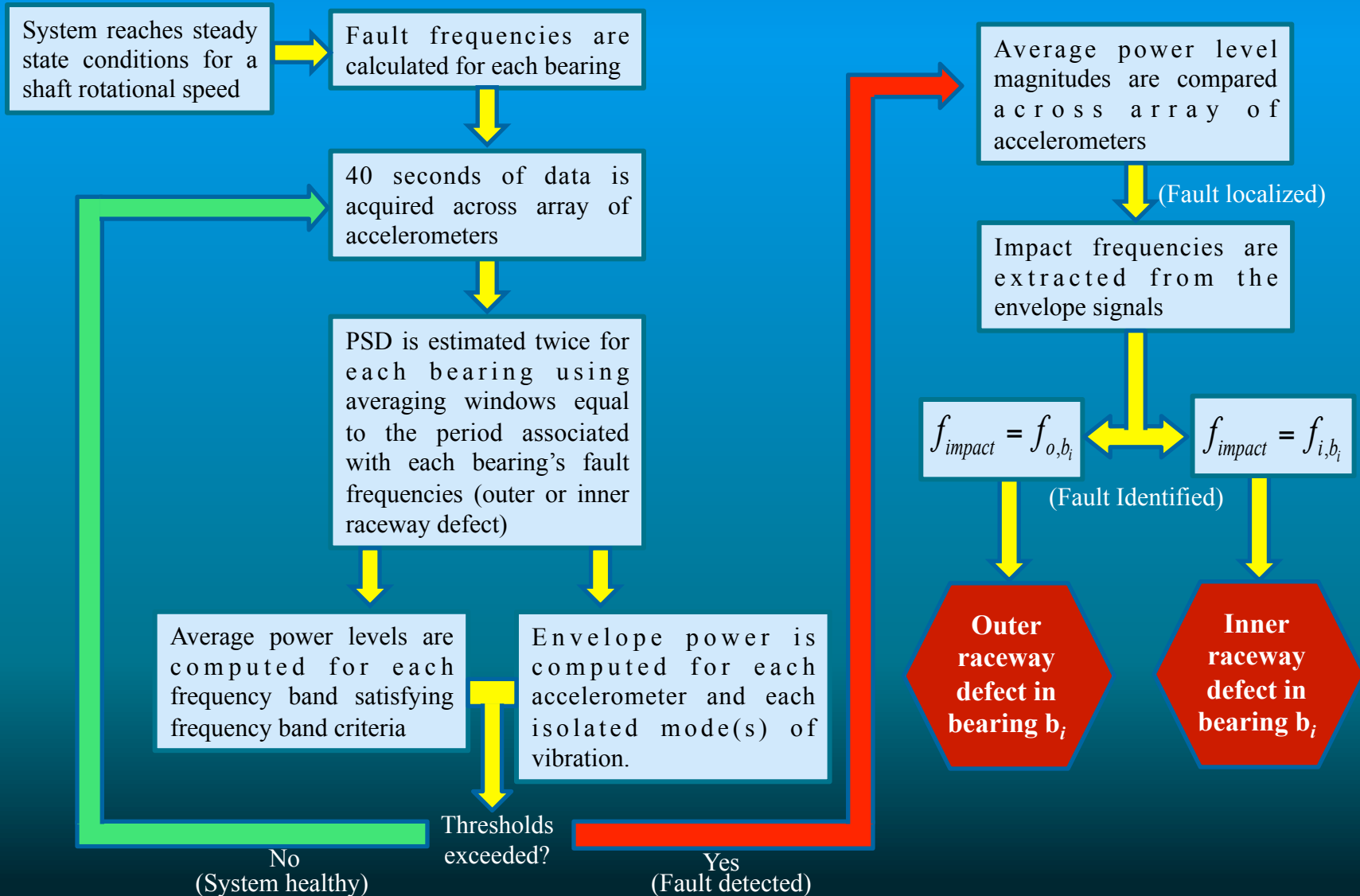
$T_{\text{impact}}$  = impact period.

$f_{o,d_{m_i}}$  = fault frequency for outer raceway defect.

$f_r$  = Shaft rotational speed.

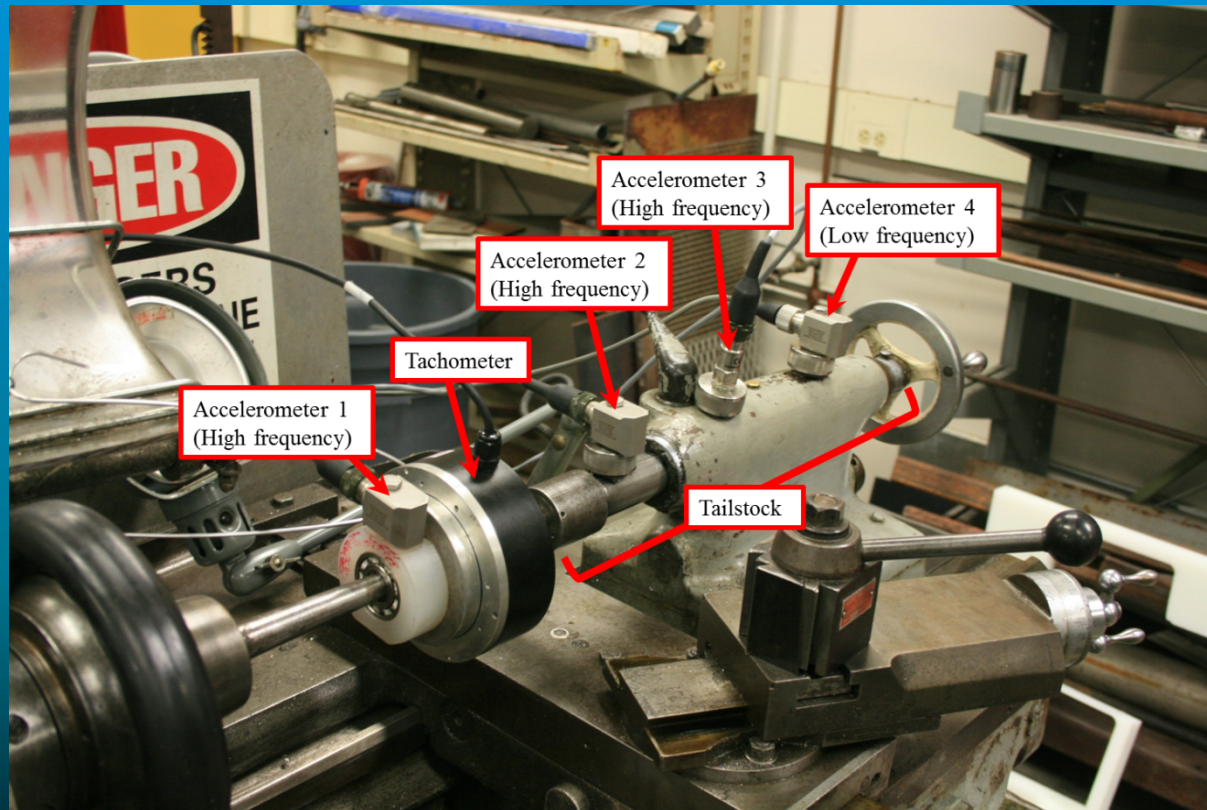
$f_{i,d_{m_i}}$  = fault frequency for inner raceway defect.

# Methodology



## Results: Experiment I

- 4 accelerometers were placed along the length of a lathe and a tachometer (for shaft rotational speed) was mounted to the shaft of the lathe.
- A collar was made for the bearings to allow for coupling different bearings to the lathe's shaft and coupling an accelerometer to the bearing.



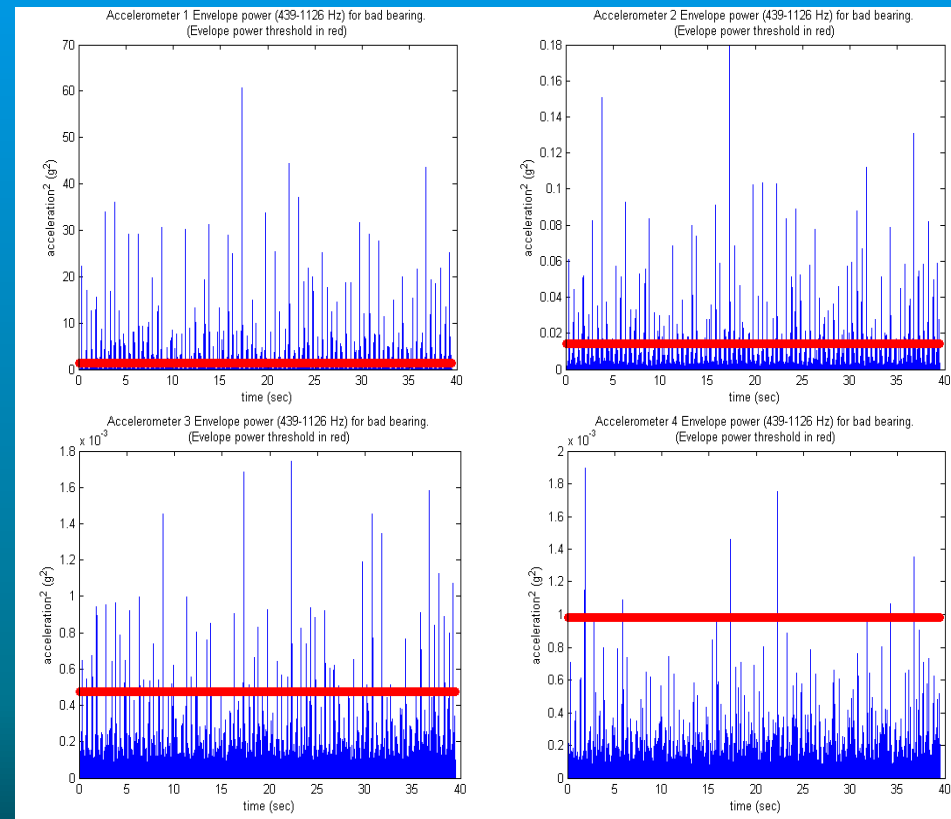
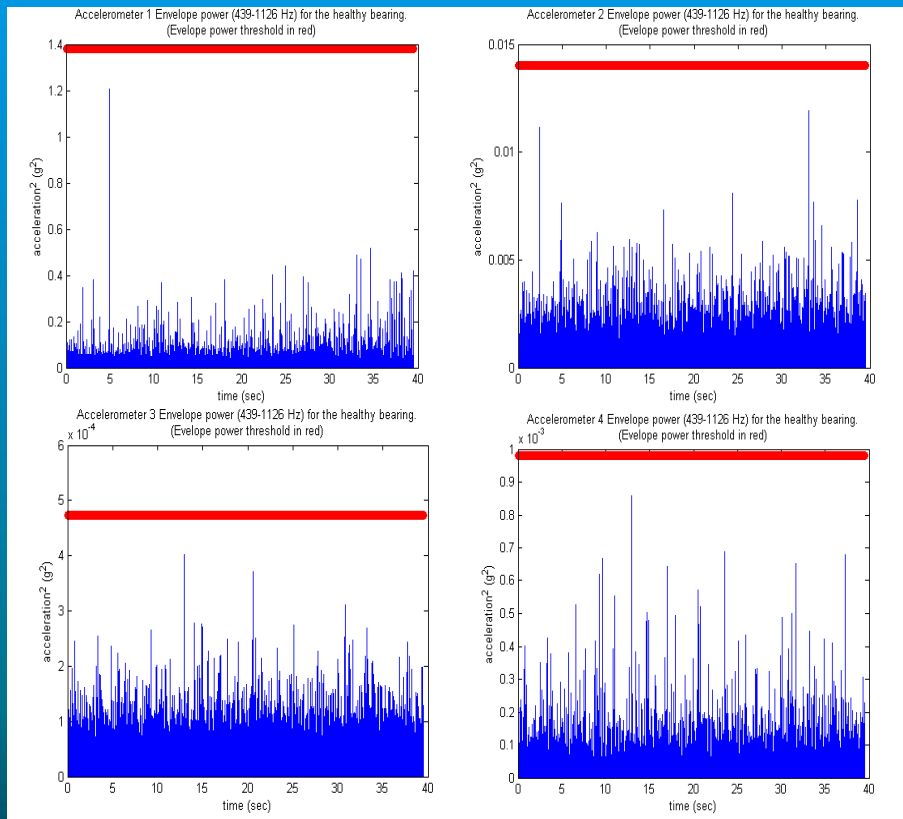
Nicholas Waters

# Results: Experiment I - Detection

- Signals from accelerometers 1-4 were demodulated about the frequency band of 439-1126 Hz.

## Healthy Bearing Envelope Power Signal.

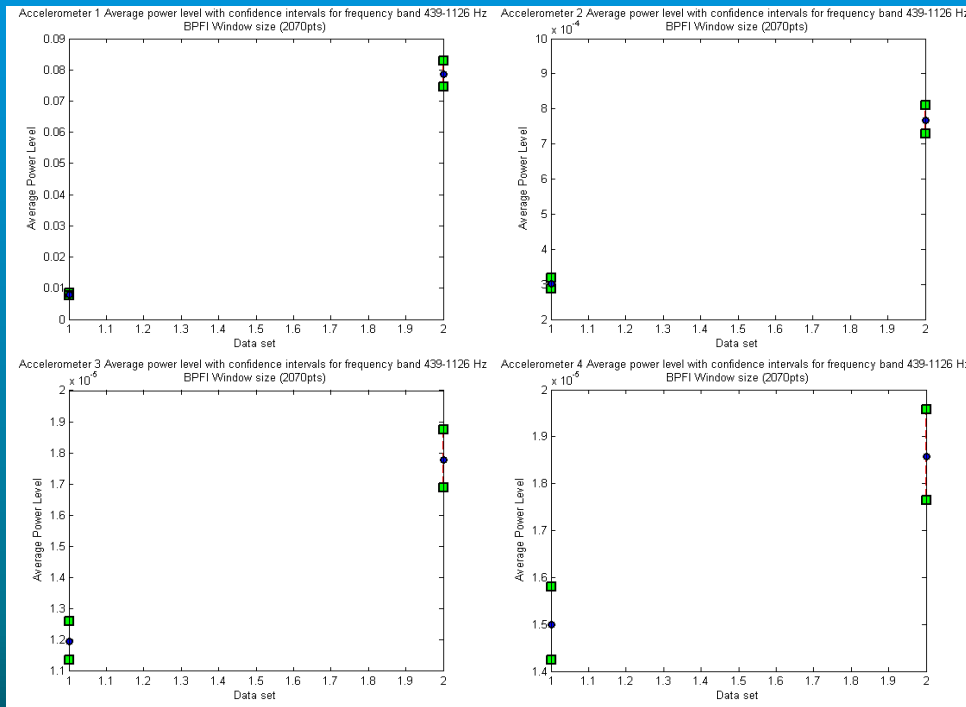
## Faulty Bearing Envelope Power Signal.



(Envelope power thresholds in red)

## Results: Experiment I - Detection and Localization

- The average power across the same frequency band (439-1126 Hz) was plotted for the entire array of accelerometers.
- An increase in average power levels across the entire array for this frequency band is apparent between the healthy and bad bearing data.



$m_i$	% Increase
1	876%
2	155%
3	49%
4	24%

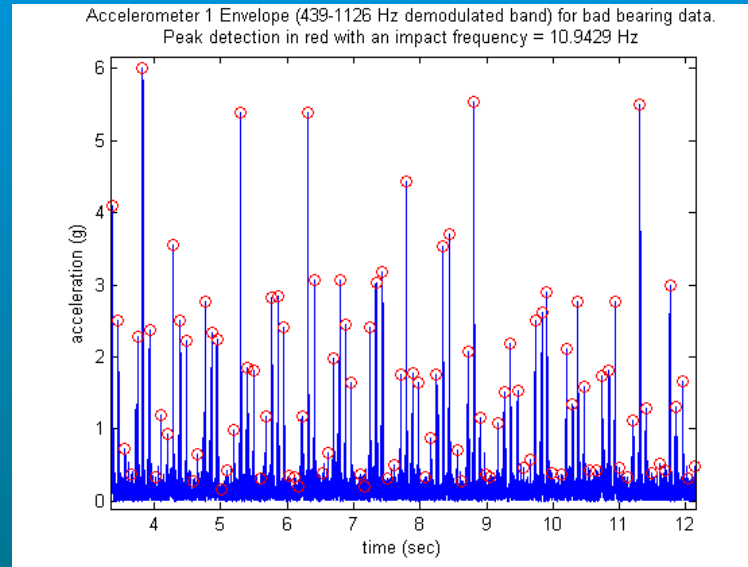
- Occurrence of fault further detected.
- Diminishing increases in average power levels, localizes fault to placement of accelerometer 1.

## Results: Experiment I - Identification

- Accelerometer 1's bad bearing data was demodulated about the 439-1126 Hz band and the envelope was extracted.
- The theoretical fault frequencies were calculated for defects along the inner and outer raceways of the bearing.

$$f_{i,b_i} = 10.86 \text{ Hz}$$

$$f_{o,b_i} = 7.14 \text{ Hz}$$



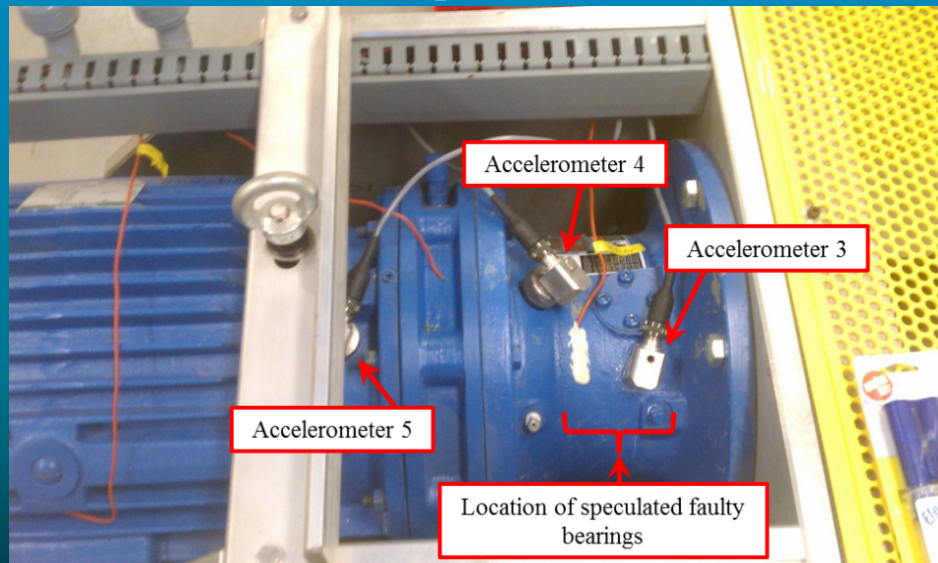
- From the envelope the period between impacts was extracted using a peak detection program.

$$f_{impact} = 10.94 \text{ Hz}$$

- Determined there was an inner raceway defect in our bearing with 0.74% error.

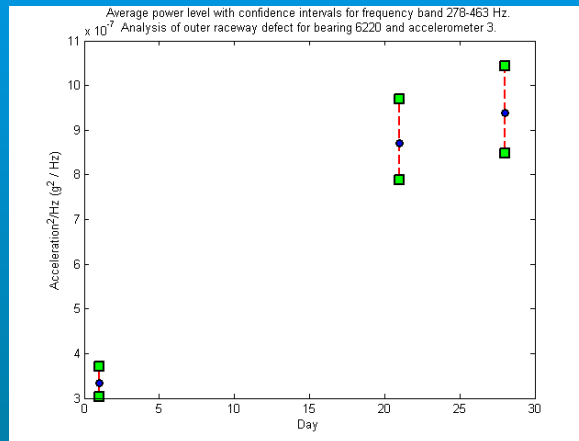
## Results

- Data collected over the course of a month were processed for two accelerometers (accelerometers 3 and 5) before the dynamometer was disassembled and the electric motor was sent for maintenance and repair.
- Shortly before the electric motor was dismantled, excessive vibrations and sound radiation were observed.
- The fault was then localized via a calibrated stethoscope to the location of two of the dynamometer's slow shaft bearings, leading us to believe that either of these bearings could contain a defect and need to be replaced.

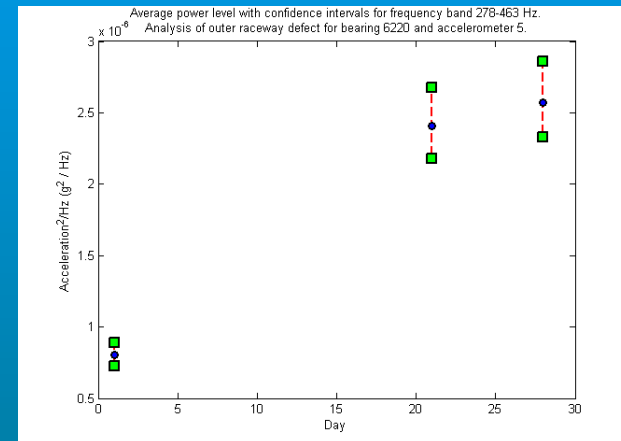


## Results

- In processing the data collected prior to detecting the fault, we found an upward trend in the average power across the frequency band of 278-463 Hz.



Average power level for accelerometer 3 with respective confidence intervals.

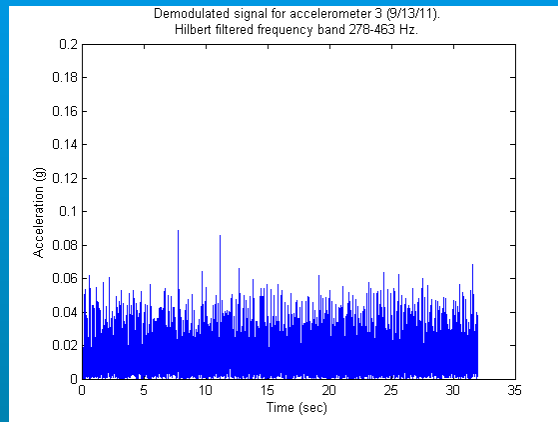


Average power level for accelerometer 5 with respective confidence intervals.

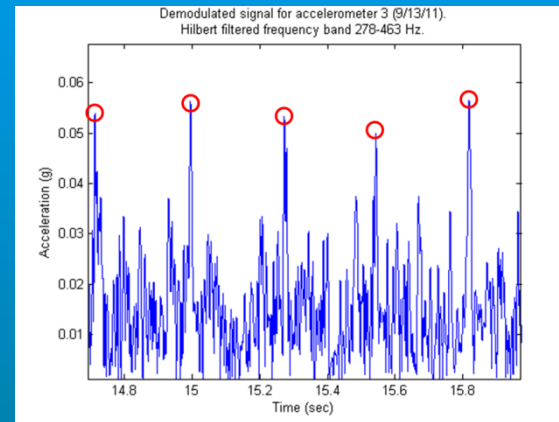
- Within this frequency band, the data acquired by accelerometer 3 showed an increase in average power level of approximately 297% in four weeks, while accelerometer 5 showed an increase of approximately 321% over the same time period.

## Results

- The signal acquired by accelerometer 3 (the accelerometer closest to the speculated fault) was demodulated using the same frequency band of 278-463 Hz for last day's data set.



Envelope of signal acquired by accelerometer 3.



Zoomed in portion of the envelope of the signal acquired by accelerometer 3 showing periodic impacts.

- The envelope of accelerometer 3's signal showed periodic impacts whose frequency of occurrence was around 3.62 Hz (Figure on right).
- The impact frequencies that we would expect to see for an inner raceway defect within either of the dynamometer's bearings that are mounted to the slow shaft (directly below accelerometer 3) are 3.41 Hz and 3.8 Hz.

## Conclusion

---

- The process of analyzing vibrations across an array of accelerometers in order to specifically target bearing raceway defects occurring in real-time on a dynamometer has been presented.
- Through trending of the average power across specific frequency bands, the presence of a faulty bearing is detected.
- Envelop power levels are compared against healthy operating conditions as another method to detect the occurrence of a bearing fault.
- By comparing the average power levels across the array of accelerometers for each frequency band, localization of the defect to the position of the accelerometer with the highest average power level is accomplished.
- The exact bearing containing the fault is identified by observing periodic impacts in the envelope signal and matching this frequency to the calculated fault frequency for one of the bearings.
- This method of bearing fault detection, localization, and identification has been demonstrated in a near ideal scenario (Lathe experiment) and on data collected from the dynamometer leading up to a bearing failure.

*THANK YOU*